PHYSICAL REVIEW B **78**, 020511(R) (2008)

# First-order-type effects in $YBa_2Cu_3O_{6+x}$ at the onset of superconductivity

L. Tassini, W. Prestel, A. Erb, M. Lambacher, and R. Hackl
*Walther Meissner Institut, Bayerische Akademie der Wissenschaften, 85748 Garching, Germany*
(Received 16 June 2008; published 29 July 2008)

We present results of Raman-scattering experiments on tetragonal $(Y_{1-y}Ca_y)Ba_2Cu_3O_{6+x}$ for doping levels $p(x,y)$ between 0 and 0.07 holes/$CuO_2$. Below the onset of superconductivity at $p_{sc1}\approx 0.06$, we find evidence of a diagonal superstructure. At $p_{sc1}$, lattice and electron dynamics change discontinuously with the charge and spin properties being renormalized at all energy scales. The results indicate that charge ordering is intimately related to the transition at $p_{sc1}$ and that the maximal transition temperature to superconductivity at optimal doping $T_c^{max}$ depends on the type of ordering at $p>p_{sc1}$.

DOI: 10.1103/PhysRevB.78.020511 PACS number(s): 74.72.−h, 74.20.Mn, 74.25.Gz, 78.30.−j

In cuprates the maximal transition temperature to superconductivity $T_c^{max}$ depends on the compound class. In contrast, the variation of $T_c$ with doping $p$ does not, and superconductivity exists between approximately 0.05 and 0.27 holes per $CuO_2$ formula unit in clean samples.[1] In the presence of disorder this range shrinks[1] leading to a sample-specific onset point of superconductivity at $p_{sc1}\geq 0.05$. In addition to superconductivity, short-range antiferromagnetism with the domains separated by quasi-one-dimensional charged stripes can occur.[2–6] In $La_{2-x}Sr_xCuO_4$ $(p=x)$, this superstructure is oriented along the diagonals of the $CuO_2$ plane below $p_{sc1}$ and rotates by 45° at $p_{sc1}$ (Ref. 7). This rotation was also seen in the low-energy electronic Raman spectra where the ordering-related response flips symmetry.[8]

For $p>p_{sc1}$, superstructures are observed in all cuprates.[3,6,9–12] However, the type of ordering and its relationship to superconductivity is rather complicated to pin down.[5,13,14] In a few compounds the lattice stabilizes static spin and charge superstructures and the superconducting transition temperature is reduced or quenched.[3,6] In most of the cases, fluctuating order prevails and it is particularly hard to detect the charge part.[5,13] Raman spectroscopy was found to be a viable method.[8]

Inelastic (Raman) scattering of light is capable of probing most of the excitations in a solid including lattice vibrations, spins, and electrons, as well as their interactions.[15] Since the polarizations of the incident and the scattered photons can be adjusted independently, many of the excitations can be sorted out via the selection rules. For instance, the transport properties of conduction electrons can be measured independently in different regions of the Brillouin zone,[15,16] and the orientation of (fluctuating) charged stripes can be determined.[8] A detailed model calculation[17] demonstrated that in addition to the symmetry selection rules, the dependence on energy and temperature of the response related to stripes can be understood quantitatively (Fig. 1) in terms of charge-ordering fluctuations.

In this Rapid Communication, we focus on the "high-$T_c$" compound $YBa_2Cu_3O_{6+x}$ (Y-123) at doping levels $0\leq p\leq 0.07$. The purpose is to gain an insight into the nature of the onset of superconductivity at $p_{sc1}\approx 0.06$ and into possible discrimination criteria to the "low-$T_c$" compound $La_{2-x}Sr_xCuO_4$ (LSCO) studied earlier.[7,8,17] For $0<p<p_{sc1}$, we find spectral features strikingly similar to those of LSCO and conclude that the diagonal stripelike superstructure is universal. Above $p_{sc1}$, the indications of the diagonal superstructure disappear. However, in clear contrast to LSCO no indications of stripe ordering are found in Y-123. Hence, the first-order-type changes at $p_{sc1}$ are not a peculiarity of LSCO (Ref. 7 and 8) but exist also, although with distinct differences, in Y-123. Along with that, the direct spin-spin exchange interaction and the electron-phonon coupling discontinuously decrease and increase, respectively, across $p_{sc1}$.

For the studies we used single crystals of $(Y_{1-y}Ca_y)Ba_2Cu_3O_{6+x}$ grown in $BaZrO_3$ crucibles.[18] Doping with Ca allows us to directly control the number of holes. For $x\simeq 0$, doping levels up to $p=0.06$ are given by the Ca content $p=y/2$ (Ref. 1). Crystals with 0, 2, 8, and 12% Ca were studied, all are not superconducting for $x\simeq 0$. Superconductivity could be induced only by oxygen codoping ($y=0.08$, $x=0.3$), and $p\simeq 0.07$ is estimated from the transition temperature $T_c=28$ K via the universal relationship $T_c(p)$ (Ref. 1). The material remains tetragonal on the average. Hence, all samples studied here have the same crystal-

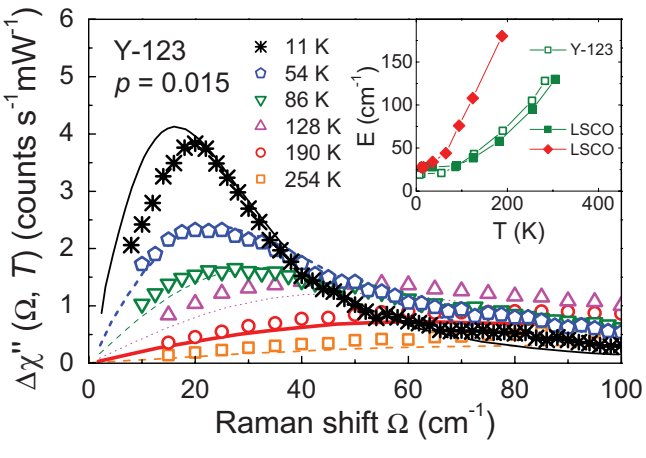


FIG. 1. (Color online) Response of charge-ordering fluctuations in $(Y_{0.97}Ca_{0.03})Ba_2Cu_3O_{6.05}$ (Ref. 17). The points represent the experimental results and the full lines are the theoretical fits. (Reproduced with permission.) Two fluctuations with finite but opposite momenta are exchanged (Azlamazov-Larkin diagrams). The inset shows the peak positions of the response as a function of temperature in $(Y_{0.97}Ca_{0.03})Ba_2Cu_3O_{6.05}$, $La_{1.98}Sr_{0.02}CuO_4$, and $La_{1.90}Sr_{0.10}CuO_4$. At similar doping $(p\simeq 0.02)$ the points essentially coincide.

 

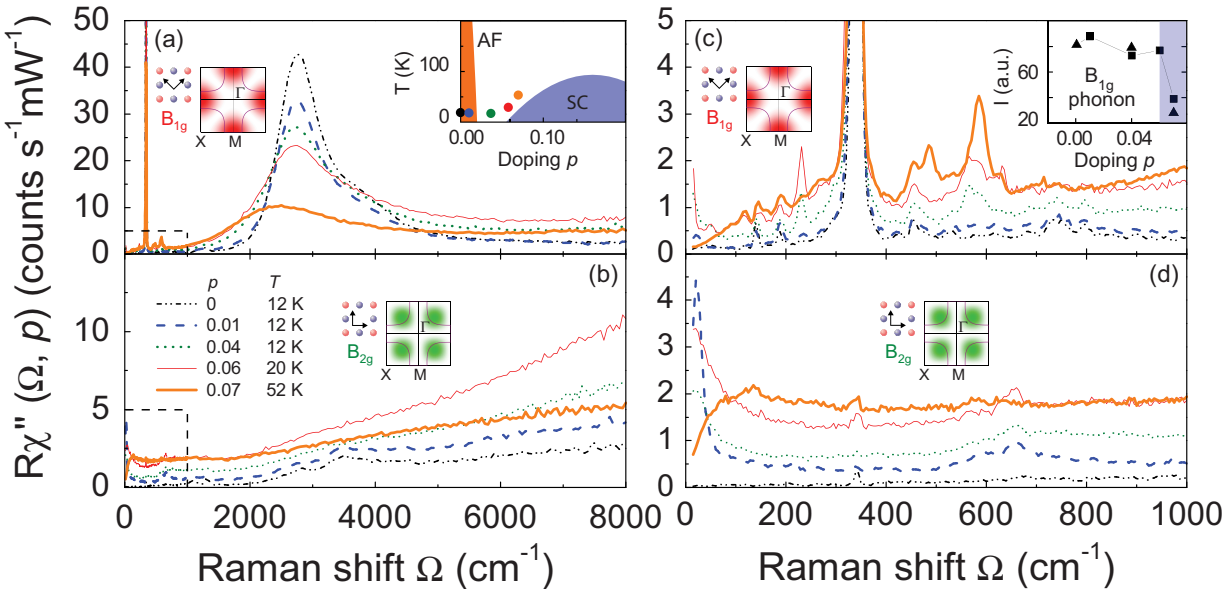


FIG. 2. (Color online) Raman response $R\chi''(p,\Omega)$ of $(Y_{1-y}Ca_y)Ba_2Cu_3O_{6+x}$ at low doping and temperature outside the superconducting state (raw data). The response $R\chi''(\Omega,p)$ is obtained by dividing the experimental spectra by the Bose factor. All spectra are measured with the Ar laser line at 458 nm. The upper (a,c) and lower (b,d) panels correspond to the $B_{1g}$ and $B_{2g}$ symmetries, respectively, with the related polarizations and sensitivities in the Brillouin zone as indicated. Doping level and measuring temperatures of the samples are shown as full circles in the schematic phase diagram in the inset in (a), where AF and SC label antiferromagnetism and superconductivity, respectively, and are indicated explicitly in (b). Panels (a) and (b) show an energy range of 8000 $cm^{-1}$ equivalent to 1 eV. In (c) and (d) the low-energy and -intensity ranges are expanded as indicated by dashed boxes in (a) and (b). The inset in (c) shows the peak intensity of the $B_{1g}$ "buckling" phonon at 340 $cm^{-1}$ (43 meV). Triangles and squares represent Ca-free and Ca-doped Y-123, respectively.

lographic structure. We made sure that the observed effects are independent of the way of doping by also studying Ca-free crystals with $x=0.3$ and 0.4 with $T_c=0$ and 26 K, respectively [see Ref. 19 and inset of Fig. 2(c)]. For $x=0.4$, the superconducting sample is orthorhombic with the twin boundaries visible under polarized light. The results are identical to within the experimental uncertainty and will be published elsewhere.

In Fig. 2 we show normal-state Raman spectra of Y-123 at low temperature in the doping range $0 \leq p \leq 0.07$. We describe first the overall trends in the energy range of 8000 $cm^{-1}$ (1 eV).

In $B_{1g}$ symmetry [Fig. 2(a)] an intense phonon at 340 $cm^{-1}$ and scattering from nearest-neighbor spin-flip excitations in the range between 2000 and 4000 $cm^{-1}$ are the most prominent features observed. The evolution with doping of the magnetic scattering shows features beyond those found before.[20,21] As long as the doping is below the onset point of superconductivity ($p \leq p_{sc1}$) the peak height changes slowly and continuously while the position is essentially constant. Upon crossing $p_{sc1}$ the two-magnon peak moves discontinuously downward by approximately 250 $cm^{-1}$. Independent of doping, positions and intensities of the two-magnon peaks react only mildly when the temperature is raised.[19]

In $B_{2g}$ symmetry [Fig. 2(b)] light scattering from spin excitations is weak.[15] A low-energy continuum appears only at finite carrier concentrations. The high-energy response increases continuously until superconductivity sets in. Then, the spectrum assumes a more convex shape and is depressed at high energy.

Zooming in on low energies [Figs. 2(c) and 2(d)] we observe a continuous increase in the electronic response upon doping in $B_{1g}$ symmetry [Fig. 2(c)] with no significant changes across $p=p_{sc1}$. On the other hand, the peak height of the $B_{1g}$ phonon at 340 $cm^{-1}$ collapses by a factor of two for $p > p_{sc1}$ [inset of Fig. 2(c)].

In $B_{2g}$ symmetry [Fig. 2(d)] we find a complete suppression of the electronic Raman spectra below 400 $cm^{-1}$ for $p=0$ as expected for an insulator. As soon as carriers are added the response becomes finite and a new peak in the range of 15–30 $cm^{-1}$ pops up similar to those in $La_{1.98}Sr_{0.02}CuO_4$ (Ref. 8) and $(Y_{0.97}Ca_{0.03})Ba_2Cu_3O_{6.05}$ (Fig. 1 and Ref. 17). Up to $p_{sc1}$ the integrated cross section increases proportional to $p$. For $p=0.07$ it does not change any further.

In Fig. 3 we plot the low-energy $B_{2g}$ spectra at two characteristic doping levels below and above $p_{sc1}$ as a function of temperature in order to further highlight the qualitative changes across the critical doping. At $p=0.07$ the response develops as expected from the resistivity and the results at $p \geq 0.1$ (Refs. 16, 22, and 23) including a pseudogap of approximately 1000 $cm^{-1}$ opening up below 150 K (Ref. 16). As shown in the inset of Fig. 3(a) the Raman relaxation rate $\Gamma_0(T) \propto (\partial\chi''/\partial\Omega)^{-1}_{\Omega=0}$ at low energies follows the resistivity when properly converted.[16] This is in clear contrast to the nonsuperconducting sample at $p=0.04$ where a qualitative difference between the Raman and the transport resistivities is found in the entire temperature range [inset of Fig. 3(b)]. As can be seen in the main panel of Fig. 3(b) the discrepancy originates from the low-energy peak developing below approximately 250 K. Along with the peak a pronounced pseudogap of approximately 650 $cm^{-1}$ opens up which, if

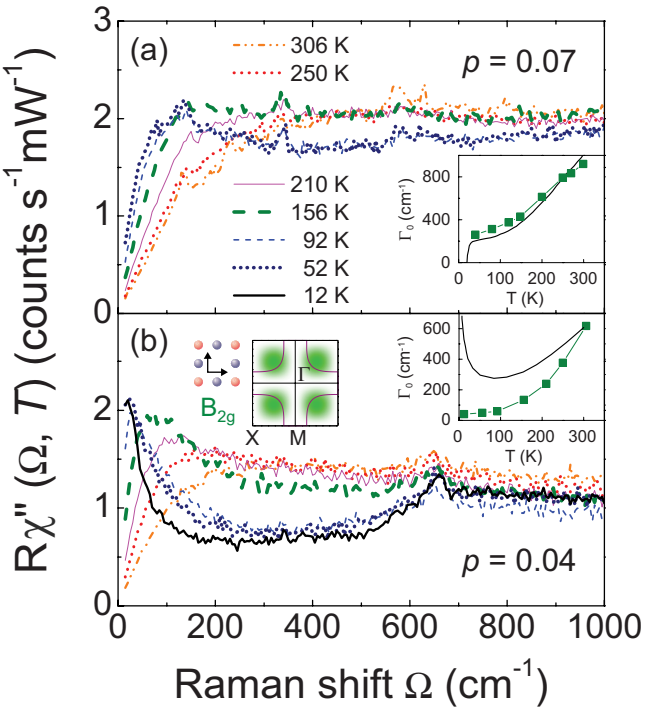


FIG. 3. (Color online) Raman responses $R\chi''_{B_{2g}}(T,\Omega)$ of $(Y_{1-y}Ca_y)Ba_2Cu_3O_{6+x}$ at $p=0.07$ (a) and 0.04 (b). In the insets we plot the low-energy "Raman resistivities" $\Gamma_0(T) \propto (\partial\chi''/\partial\Omega)^{-1}_{\Omega=0}$ (squares) corresponding to the initial slope of the spectra (Ref. 16) and compare them with the conventional resistivities (lines) from Ref. 22.

taken alone, could essentially account for the increase in the conventional resistivity toward low temperature. The pivotal question is as to what drives the abrupt changes versus doping level in the magnon, charge, and phonon spectra. In what follows we show that these changes are related to the superstructure in a universal way. So far, the rotation at $p \simeq p_{sc1}$ of the essentially one-dimensional (1D) or stripelike pattern from diagonal to parallel with respect to the Cu-O bond direction is only established in LSCO (Ref. 7), for which $T_c^{max} \simeq 40$ K. In the compounds with $T_c^{max}$ in the 100 K range, evidence of ordering is found only at $p \geq 0.10$. In Y-123 (Refs. 10 and 11) and $Bi_2Sr_2CaCu_2O_{8+\delta}$ (Ref. 9), the order is more of checkerboard or two-dimensional (2D) rather than of 1D or stripe type. For $p_{sc1} < p < 0.1$, the superstructure in Y-123 seems to disappear.[24] Very recently, nematic order was proposed to occur close to $p \simeq 0.07$ (Ref. 12). To our knowledge, there are no experiments below $p_{sc1}$.

Here, we find collective modes in the Raman spectra at $0 < p < p_{sc1}$ exhibiting shapes as well as symmetry and temperature dependences similar to those in LSCO (Ref. 8). Apparently, they originate from the same fluctuating spin and charge superstructures with a modulation along the diagonals of the $CuO_2$ plane (Fig. 1).[17] We are aware that our information is not on the structure directly but only via the dynamics. However, there is no structural analysis available and the selection rules are a particularly strong argument as to symmetry breaking and orientation. In addition, shape and temperature dependences demonstrate the similarity of the underlying physics (Fig. 1). Hence, we find indications of spin and charge orderings in a completely tetragonal cuprate in the doping range between the antiferromagnet and the onset of superconductivity. The type of ordering at $0 < p < p_{sc1}$ is universal and depends neither on the material class nor on structural details of the crystals such as lattice distortions nor on the way of doping. In fact, Ca and O doping in Y-123 lead to equivalent results[19] [for the $B_{1g}$ phonon see inset of Fig. 2(c)]. In particular, Ca is sitting on a site with the full lattice symmetry and does not trap charges.[25] Therefore, the influence on the direction of the superstructure is expected to be weaker than that of Sr in LSCO (Ref. 26) if not negligible. Alternatively, the shape of the Fermi surface can influence the orientation of the ordering in a fashion similar to nesting in materials with charge-density waves.[27] With increasing doping the distance between the stripes decreases[6,7] and the ordering wave vector $\mathbf{q}_{charge}$ becomes large enough to connect the flat parts of the underlying Fermi surface [see, e.g., inset of Fig. 2(c)]. Therefore, diagonal order becomes less favorable for phase-space reasons and disappears above $p_{sc1}$. Defects may shift $p_{sc1}$ (Ref. 1).

While symmetry arguments and analogies lead to straightforward conclusions for $p < p_{sc1}$ the analysis at $p > p_{sc1}$ is

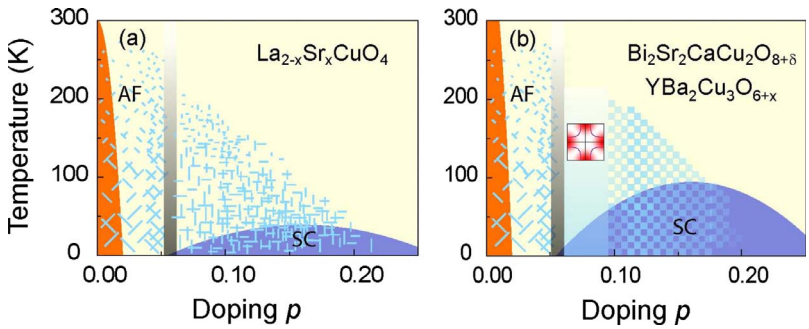


FIG. 4. (Color online) Phase diagrams for "low"- (a) and "high"-$T_c$ (b) cuprates as derived from the earlier (Ref. 8) and present Raman data and from the neutron scattering (Refs. 6, 10, 11, and 24) and scanning tunneling microscopy (Refs. 5 and 9) measurements. The position of the onset point of superconductivity $p_{sc1}$ depends on the degree of disorder with the minimum at approximately 0.05 for clean materials (Ref. 1). The lines of different length qualitatively indicate doping and temperature ranges, density, orientation, and correlation lengths of stripes. The square pattern symbolizes checkerboard order which, however, is only established for $p > 0.10$. For $p_{sc1} < p < 0.10$, there are indications from the Raman results presented here for an interaction with structure in momentum space as sketched.

less direct. In contrast to LSCO, where the ordering-induced collective modes change symmetry from $B_{2g}$ to $B_{1g}$ along with the rotation of the superstructure,[8] we do not observe any ordering-related peaks in Y-123 for $p > p_{sc1}$ [see Fig. 2(c), $p=0.07$, and Ref. 8]. However, all the renormalization effects described above demonstrate indirectly a very strong interaction peaked close to the M points, i.e., with $|d_{x^2-y^2}|$ symmetry, [see inset of Fig. 2(c)] to become effective at $p > p_{sc1}$. This interaction leads to a shift of the two-magnon peak indicating a reduction in the Heisenberg exchange coupling $J$ by almost 10%. The related fluctuations open an additional coupling channel of proper symmetry for the $B_{1g}$ phonon as indicated by the discontinuous reduction in the peak intensity and the onset of a (weak) Fano-type line shape. The effect on the $\mathbf{q} \simeq 0$ Raman phonon is relatively weak in contrast to the strong coupling at $\mathbf{q}_{charge} \simeq 0.25(2\pi/a)$ (Ref. 28). In fact, it would be interesting to study the buckling and the half-breathing phonons close to the expected $\mathbf{q}_{charge}$ right above and below $p_{sc1}$.

In conclusion, superconductivity and the apparently universal diagonal order at $p < p_{sc1}$ are mutually exclusive. On the basis of the so far available results (including ours), it seems that details of the order at $p > p_{sc1}$ are crucial for $T_c^{max}$. In the "low"-$T_c$ materials such as LSCO collinear stripe order prevails.[2–4,6,7] In compounds with $T_c$-$s$ in the 100 K range the order is more 2D, e.g., of checkerboard or nematic type, aligned with the $CuO_2$ plane.[9–12] For $p_{sc1} < p < 0.1$, we found a strongly momentum dependent interaction which is symmetry compatible with the order at $p > 0.10$ and with the superconducting gap. Possible candidates are quasicritical fluctuations of charge stripes[29] or a fluctuating Fermi-surface deformation.[12,30] Either the electron-lattice interaction[14,26] or details of the band structure[31] can influence the order. Combining our results with the earlier ones we arrive at the phase diagrams sketched in Fig. 4.

Discussions with T. P. Devereaux, C. Di Castro, and M. Grilli are gratefully acknowledged. The project was supported by the DFG under Grants No. Ha2071/3 and No. Er342/1 via the Research Unit FOR 538.

[1] J. L. Tallon, C. Bernhard, H. Shaked, R. L. Hitterman, and J. D. Jorgensen, Phys. Rev. B **51**, 12911 (1995).
[2] S. W. Cheong, G. Aeppli, T. E. Mason, H. Mook, S. M. Hayden, P. C. Canfield, Z. Fisk, K. N. Clausen, and J. L. Martinez, Phys. Rev. Lett. **67**, 1791 (1991).
[3] J. M. Tranquada, B. J. Sternlieb, J. D. Axe, Y. Nakamura, and S. Uchida, Nature (London) **375**, 561 (1995).
[4] A. Bianconi, N. L. Saini, A. Lanzara, M. Missori, T. Rossetti, H. Oyanagi, H. Yamaguchi, K. Oka, and T. Ito, Phys. Rev. Lett. **76**, 3412 (1996).
[5] S. A. Kivelson, I. P. Bindloss, E. Fradkin, V. Oganesyan, J. M. Tranquada, A. Kapitulnik, and C. Howald, Rev. Mod. Phys. **75**, 1201 (2003).
[6] J. M. Tranquada, in *Handbook of High-Temperature Superconductivity*, edited by J. Robert Schrieffer (Springer, Heidelberg, 2007); arXiv:cond-mat/0512115 (unpublished).
[7] S. Wakimoto, G. Shirane, Y. Endoh, K. Hirota, S. Ueki, K. Yamada, R. J. Birgeneau, M. A. Kastner, Y. S. Lee, P. M. Gehring, and S. H. Lee, Phys. Rev. B **60**, R769 (1999).
[8] L. Tassini, F. Venturini, Q.-M. Zhang, R. Hackl, N. Kikugawa, and T. Fujita, Phys. Rev. Lett. **95**, 117002 (2005).
[9] J. E. Hoffman, K. M. Lang, V. Madhaven, H. Eisaki, S. Uchida, and J. C. Davis, Science **295**, 466 (2002).
[10] V. Hinkov, S. Pailhes, P. Bourges, Y. Sidis, A. Ivanov, A. Kulakov, C. T. Lin, D. P. Chen, C. Bernhard, and B. Keimer, Nature (London) **430**, 650 (2004).
[11] C. Stock, W. J. L. Buyers, R. A. Cowley, P. S. Clegg, R. Coldea, C. D. Frost, R. Liang, D. Peets, D. Bonn, W. N. Hardy, and R. J. Birgeneau, Phys. Rev. B **71**, 024522 (2005).
[12] V. Hinkov, D. Haug, B. Fauquè, P. Bourges, Y. Sidis, A. Ivanov, C. Bernhard, C. T. Lin, and B. Keimer, Science **319**, 597 (2008).
[13] C. Castellani, C. Di Castro, and M. Grilli, J. Phys. Chem. Solids **59**, 1694 (1998).
[14] H.-H. Klauss, W. Wagener, M. Hillberg, W. Kopmann, H. Walf, F. J. Litterst, M. Hücker, and B. Büchner, Phys. Rev. Lett. **85**, 4590 (2000).
[15] T. P. Devereaux and R. Hackl, Rev. Mod. Phys. **79**, 175 (2007).
[16] M. Opel *et al.*, Phys. Rev. B **61**, 9752 (2000).
[17] S. Caprara, C. Di Castro, M. Grilli, and D. Suppa, Phys. Rev. Lett. **95**, 117004 (2005).
[18] A. Erb, E. Walker, and R. Flükiger, Physica C **258**, 9 (1996).
[19] L. Tassini, Ph.D. thesis, Technical University Munich, 2008.
[20] S. Sugai, H. Suzuki, Y. Takayanagi, T. Hosokawa, and N. Hayamizu, Phys. Rev. B **68**, 184504 (2003).
[21] A. Gozar, S. Komiya, Y. Ando, and G. Blumberg, *Frontiers in Magnetic Materials* (Springer-Verlag, Berlin, 2005), p. 755.
[22] Y. Ando, S. Komiya, K. Segawa, S. Ono, and Y. Kurita, Phys. Rev. Lett. **93**, 267001 (2004).
[23] F. Venturini, M. Opel, T. P. Devereaux, J. K. Freericks, I. Tüttő, B. Revaz, E. Walker, H. Berger, L. Forró, and R. Hackl, Phys. Rev. Lett. **89**, 107003 (2002).
[24] C. Stock, W. J. L. Buyers, Z. Yamani, C. L. Broholm, J. H. Chung, Z. Tun, R. Liang, D. Bonn, W. N. Hardy, and R. J. Birgeneau, Phys. Rev. B **73**, 100504(R) (2006).
[25] A. Jánossy, T. Fehér, and A. Erb, Phys. Rev. Lett. **91**, 177001 (2003).
[26] O. P. Sushkov and V. N. Kotov, Phys. Rev. Lett. **94**, 097005 (2005).
[27] G. Grüner, *Density Waves in Solids* (Addison-Wesley, Reading, MA, 1994).
[28] D. Reznik, L. Pintschovius, M. Ito, S. Iikubo, M. Sato, H. Goka, M. Fujita, K. Yamada, G. D. Gu, and J. M. Tranquada, Nature (London) **440**, 1170 (2006).
[29] A. Perali, C. Castellani, C. Di Castro, M. Grilli, E. Piegari, and A. A. Varlamov, Phys. Rev. B **62**, R9295 (2000).
[30] W. Metzner, D. Rohe, and S. Andergassen, Phys. Rev. Lett. **91**, 066402 (2003).
[31] G. Seibold, J. Lorenzana, and M. Grilli, Phys. Rev. B **75**, 100505(R) (2007).